ESA–MOST China Dragon 4 Cooperation

# → ADVANCED TRAINING COURSE IN OCEAN AND COASTAL REMOTE SENSING

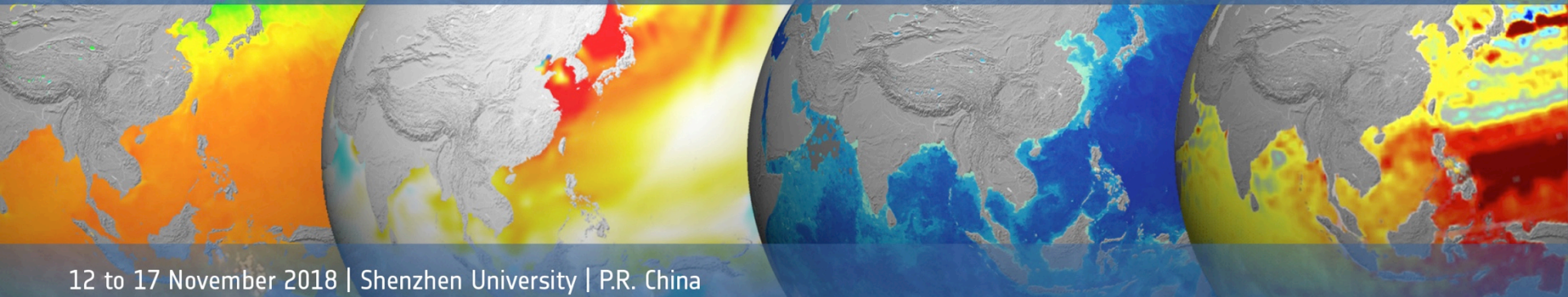

12 to 17 November 2018 | Shenzhen University | P.R. China

## “Principles of wind waves and wave current interaction from space”, Werner Alpers

Hosted by

# Imaging of ocean surface waves by SAR

**SAR imaging artifacts become significant due to motion of the sea surface**

# Real Aperture Radar (RAR) Principle

**Side-looking airborne radar = Real Aperture Radar (RAR)**

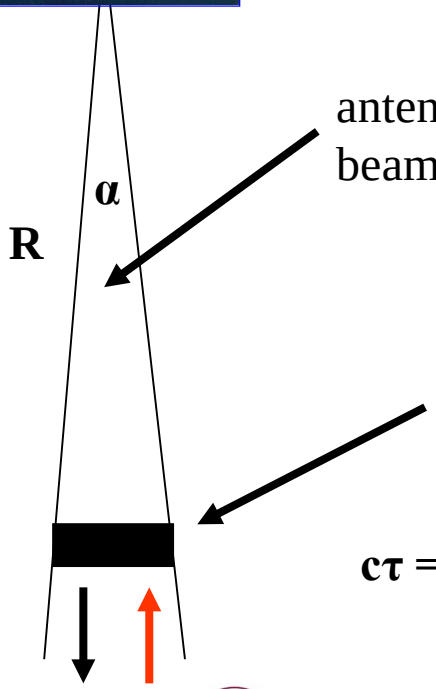


azimuth resolution:

$\rho_a = \alpha R$

$\alpha = \lambda / L$

λ = radar wavelength
L = antenna length

range resolution:

$\rho_r = c \tau / 2$

$c\tau$ = pulse length

# Synthetic aperture radar (SAR) Principle

**SAR exploits the Doppler history of the backscattered signal to achieve high azimuthal resolution**

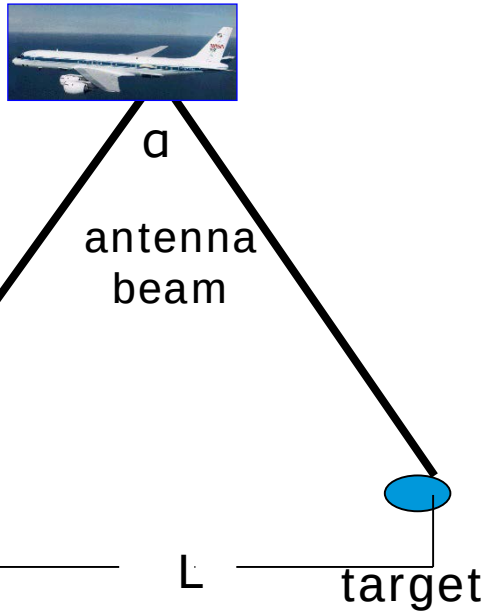


L = length of the synthetic antenna

The target is for T seconds in the antenna beam

# SAR imaging of a stationary target

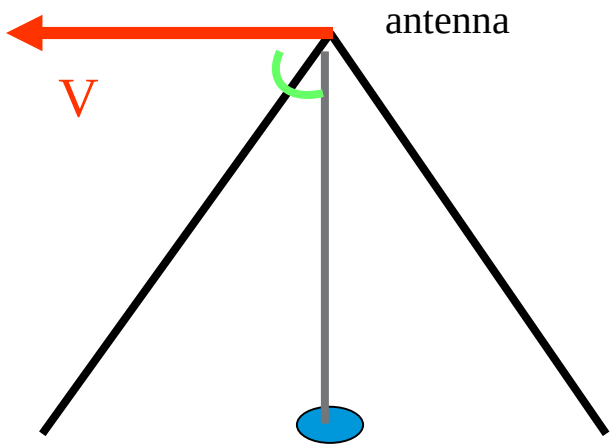


$f_d = 0$

$f_d$ = Dopplershift

The target is positioned at Doppler zero

In SAR processing, it is assumed that the targets are stationary.

When the targets (like ocean waves) are moving, then the SAR gets “confused” and generates artifacts.

# Moving train imaged by SAR

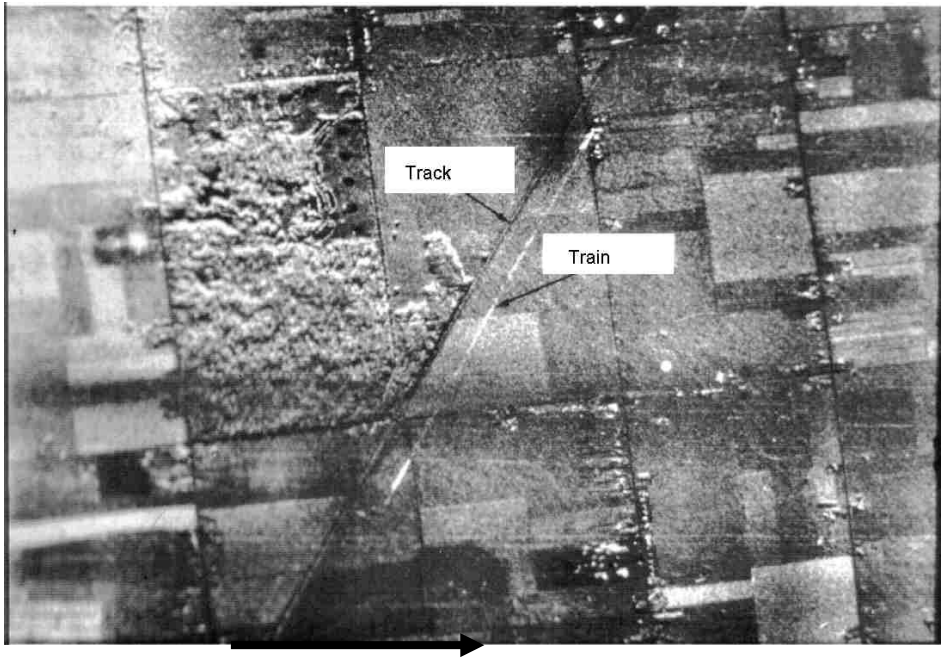


**Flight direction (or azimuth direction)**

**The train is not running on the tracks!**

# SAR imaging of a moving target

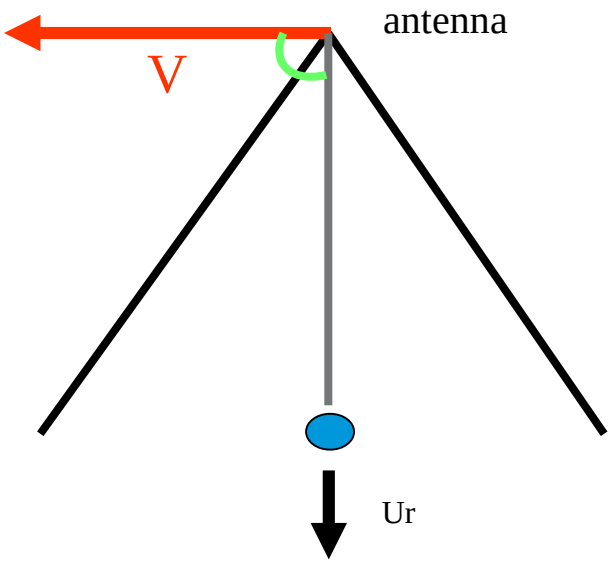


*The SAR positions the target at Doppler = zero, which is not anymore in the center of the antenna beam.*

# SAR imaging of a moving target

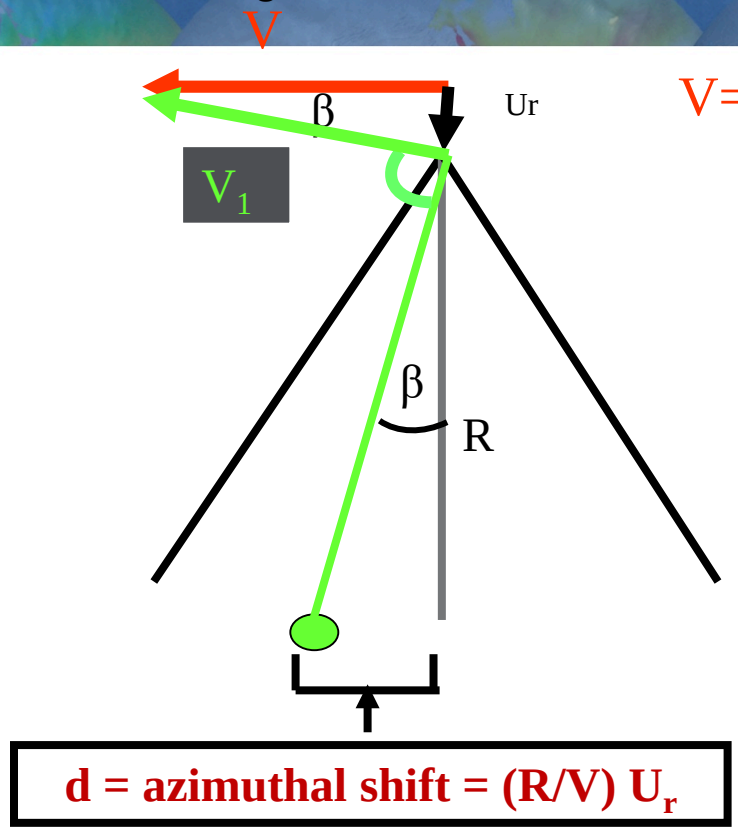


V= velocity of the platform

$U_r$ = radial component of the target velocity

$\tan \beta = \beta = U_r / V = d/R$

Doppler zero is not encountered anymore at right angle to V, but at right angle to $V_1$

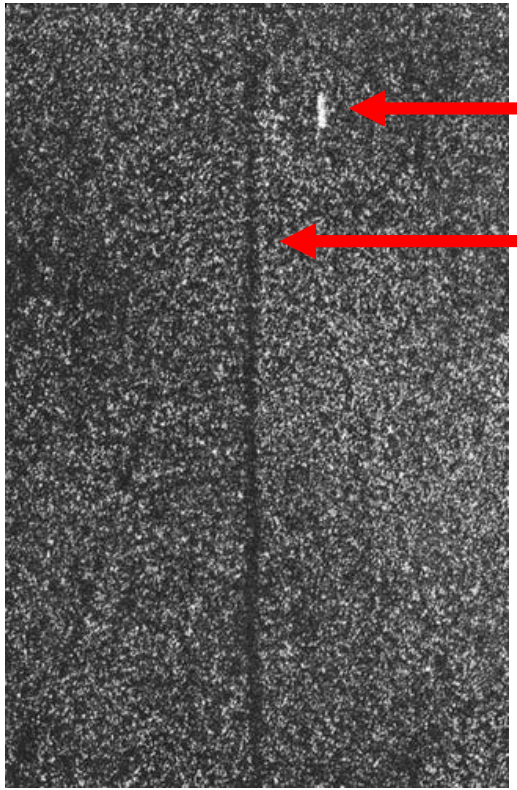


Speed of the ship:

$U_r = Vd/R$

Seasat SAR image
English Channel

Since the ocean waves cause a non-uniform motion of the water surface (the targets move back and forth), SAR can only provide a distorted image of the ocean wave field.

This is known since more than 30 years, but still ignored by many scientists.

Alpers, W.R., and C.L. Rufenach: "The effect of orbital motions on synthetic aperture radar imagery of ocean waves", *IEEE Trans. Antennas Propagat.*, AP-27, 685-690, 1979.

Alpers, W., D.B. Ross, and C.L. Rufenach: "On the detectability of ocean surface waves by real and synthetic aperture radar", *J. Geophys. Res.*, 86, 6481-6498, 1981,

# Schematic of "velocity bunching" (1979)

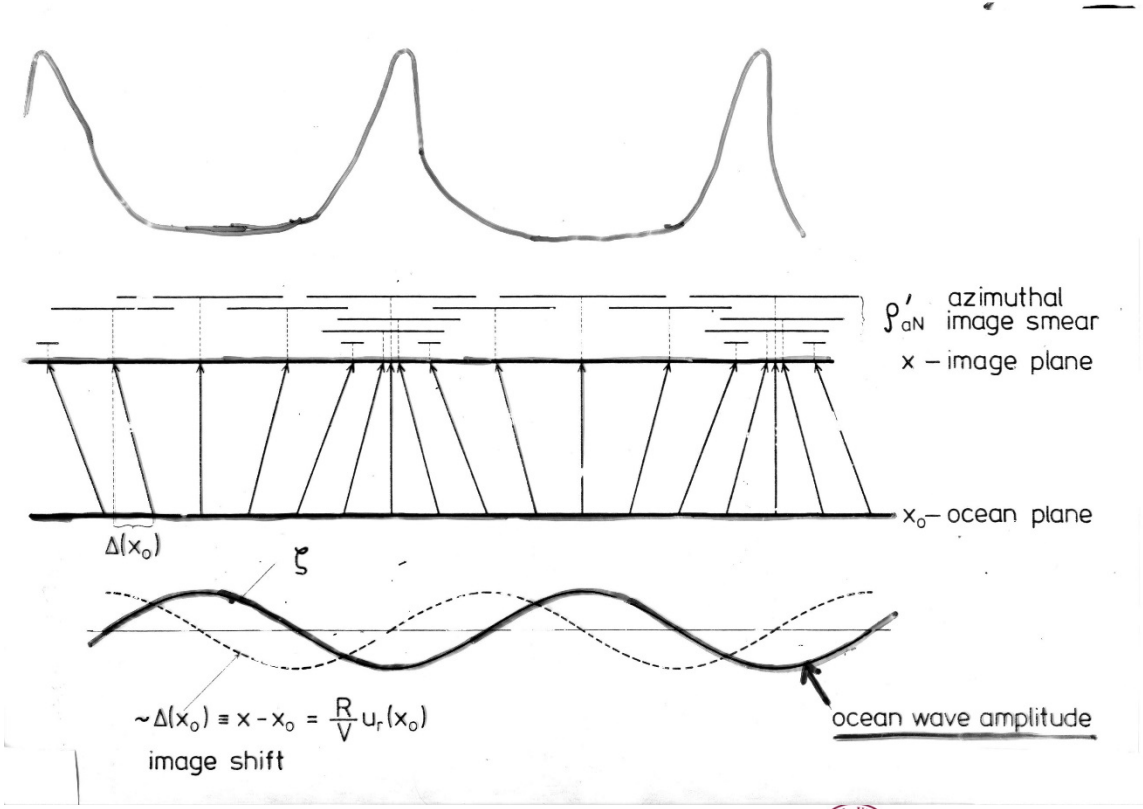


*SAR image of a sinosoidal ocean wave*

*Sinosoidal ocean wave*

**The SAR imaging of ocean waves is –in general - dominated by motion-induced effects, called**

**“velocity bunching”**

**The SAR imaging of ocean surface waves is – in - general - strongly nonlinear.**

# Simulation results

## Ocean wave field

## SAR image

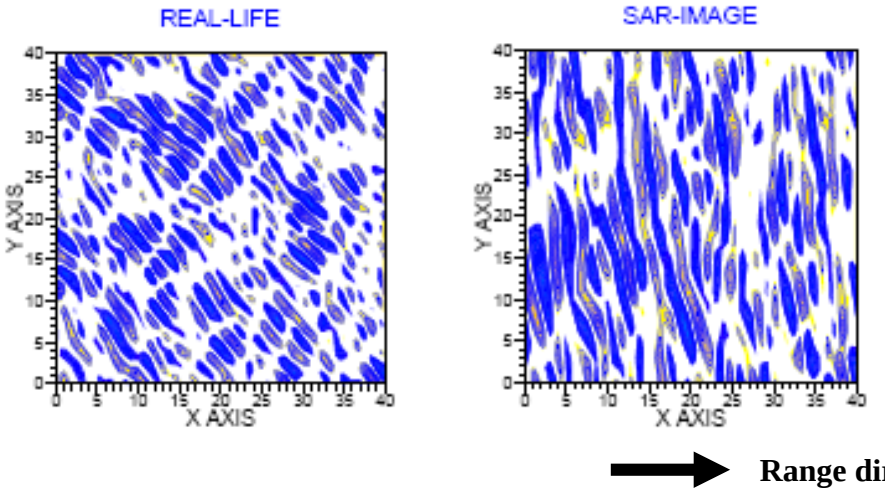


**Range direction**

***Waves are rotated in range direction by the SAR imaging mechanism***

Comparison of a sea surface elevation map with the corresponding simulated SAR image intensity map (right panels). In the left panels the corresponding ocean wave and SAR image intensity spectra are shown. Imaged is a wind sea with mean wave direction of 45 deg. from the range direction. The azimuthal cutoff wavelength is 229 m. The x-direction is the range direction (from Janssen and Alpers, 2006).

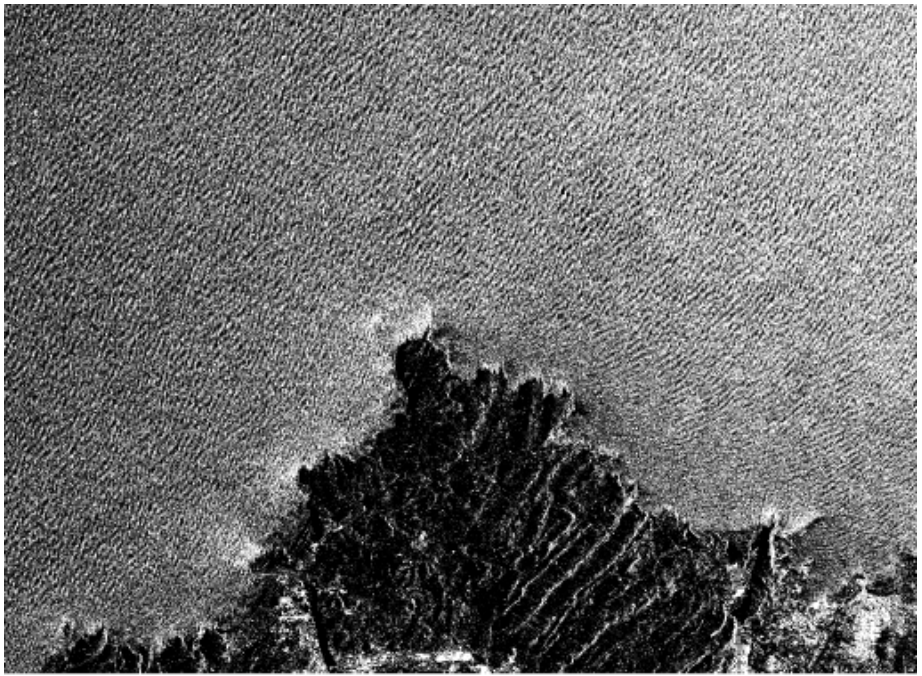

ERS-2 SAR image of surface waves (off the northern coast of Spain)

The SAR image of an ocean wave field is, in general, a highly distorted image of the ocean wave field.

However, in certain cases, the nonlinearity effect due to velocity bunching is small when swell is imaged that has long wavelength, small amplitude and travels close to the range direction.

**In this case, quasi-linear SAR imaging theory applies.**

# Waves across the Pacific revisited

*« A comparison with meteorological events in the Southern Ocean would be far more meaningful if such Observations could be made at a time when a weather satellite is in suitable orbit »* (Munk et al. 1963)

esa

Data sources:
NDBC buoys
**ENVISAT ASAR**
Altimeters
(+propagation models)

SAR is the swell instrument
-SAR wave mode products

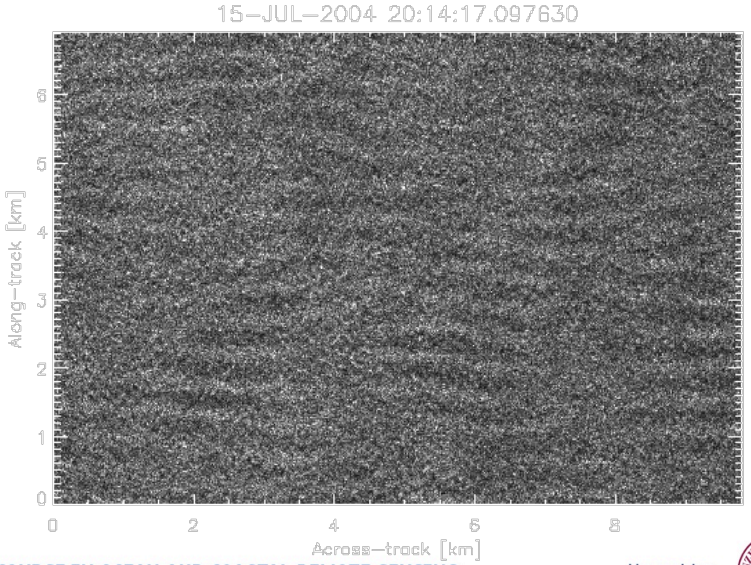


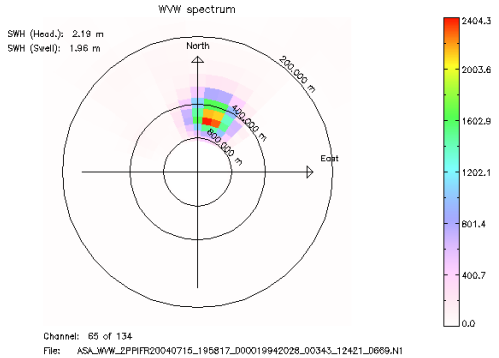

# Fireworks

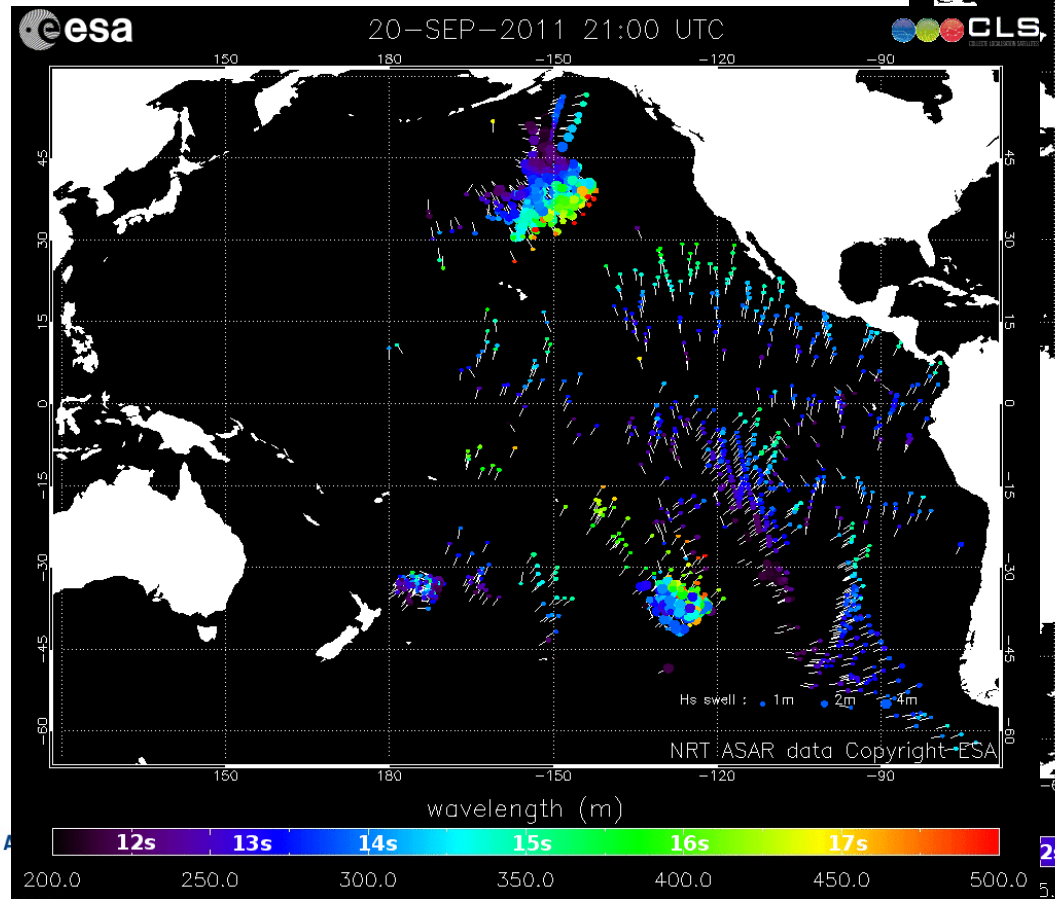
esa
20-SEP-2011 21:00 UTC
CLS
Hs swell : 1m 2m 4m
NRT ASAR data Copyright ESA
wavelength (m)
12s 13s 14s 15s 16s 17s
200.0 250.0 300.0 350.0 400.0 450.0 500.0

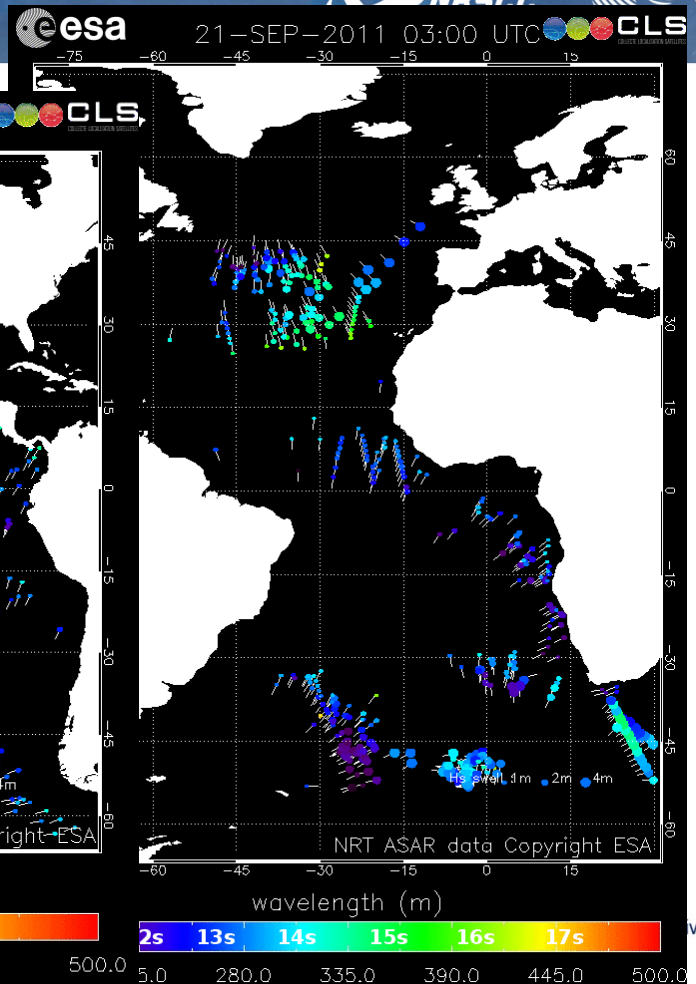
esa
21-SEP-2011 03:00 UTC
CLS
Hs swell 1m 2m 4m
NRT ASAR data Copyright ESA
wavelength (m)
2s 13s 14s 15s 16s 17s
5.0 280.0 335.0 390.0 445.0 500.0

# Swell propagating in a current field

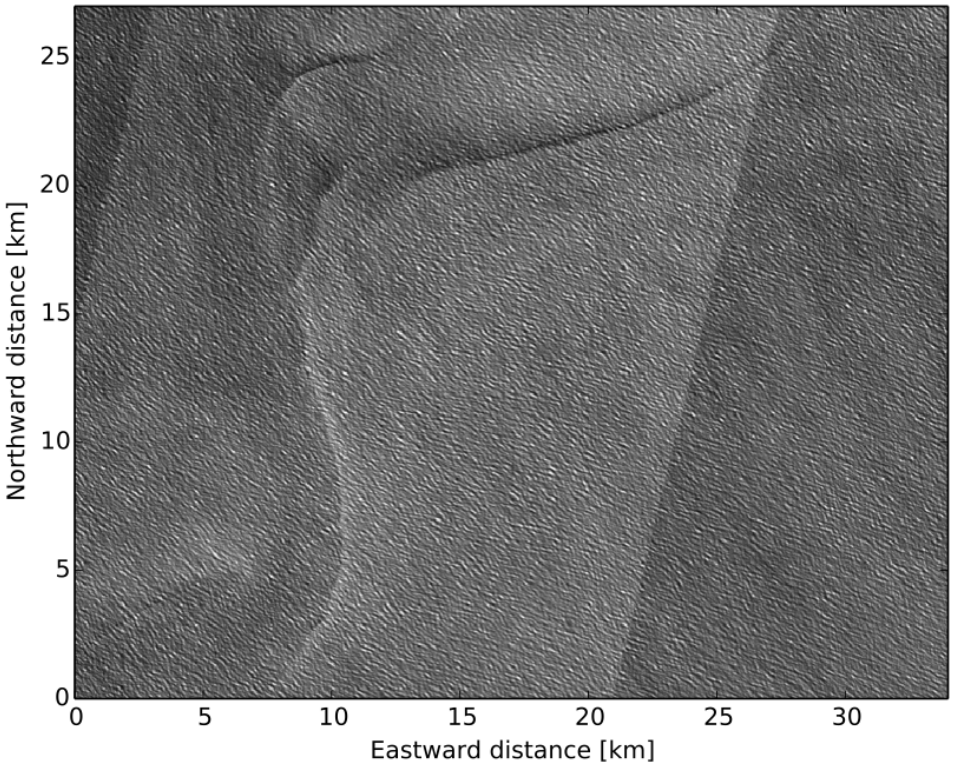


Agulhas region

The interaction of (peak) waves on deep water with spatially varying currents may be described by ray theory, with the wave amplitudes determined by the conservation of wave action .

$$\frac{\partial \theta}{\partial t} + \Omega(\boldsymbol{x}, \tilde{\nabla}\theta) = 0. \qquad \Omega = \bar{\Omega} + \boldsymbol{k} \cdot \tilde{\boldsymbol{U}}.$$

$$\frac{\mathrm{d}\bar{\boldsymbol{x}}}{\mathrm{d}t} = \Omega_{,k}(\bar{\boldsymbol{x}}, \bar{\boldsymbol{k}}), \quad \frac{\mathrm{d}\bar{\boldsymbol{k}}}{\mathrm{d}t} = -\tilde{\nabla}\Omega(\bar{\boldsymbol{x}}, \bar{\boldsymbol{k}}),$$

# CFOSAT

Since 29 October 2018, an active microwave instrument is in space, that can measure ocean wave spectra without suffering from motion effects.

CFOSAT = Chinese-French Ocean Satellite

- SWIM instrument
- Based on Real Aperture Radar Principle
- Measures directional spectra of ocean waves for wavelengths larger than about 70 m.

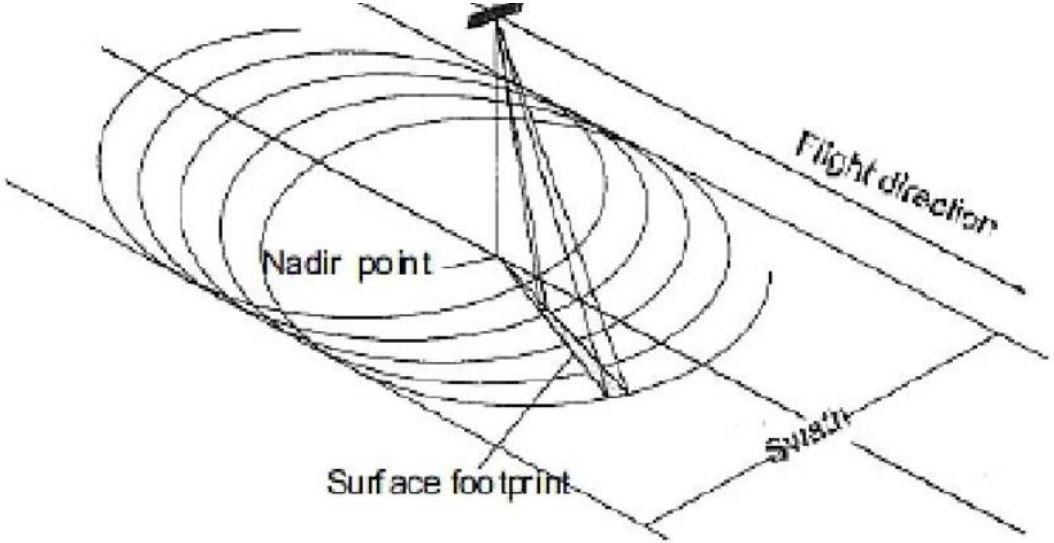


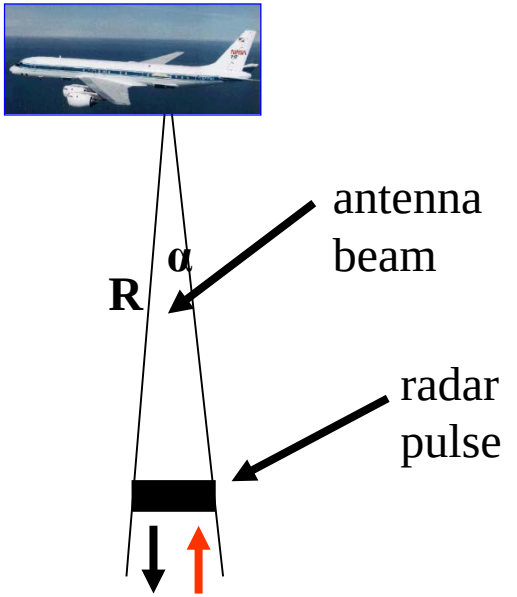


Rotating antenna with 6 incidence angles: 0°, 2°, 4°, 6°, 8° and 10°.

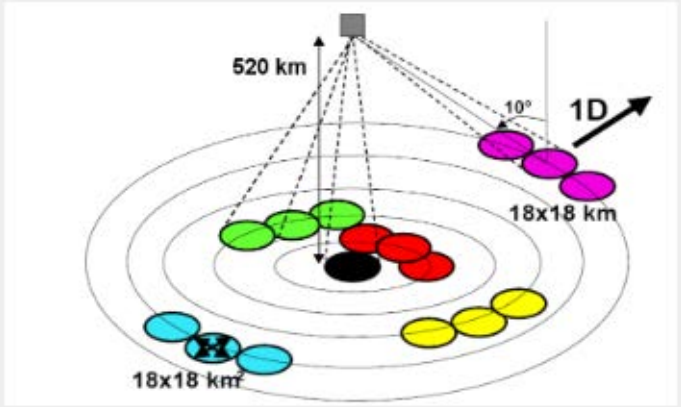


Geometry of observations of SWIM

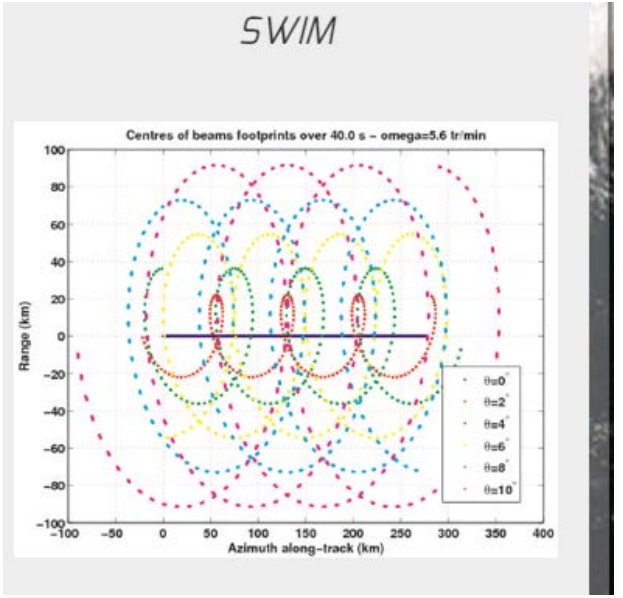


*Surface patterns described by the SWIM antenna beams for an orbit altitude of 500 km*

# First results

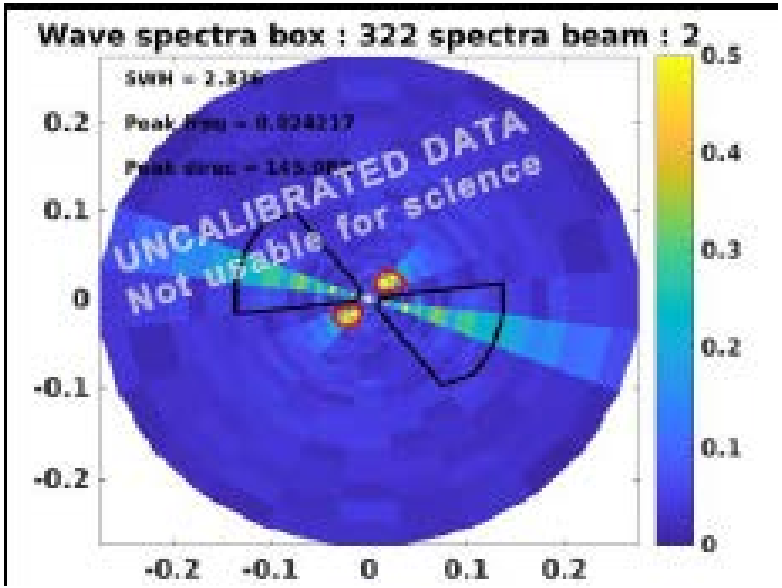

# SAR imaging of current features

is based on current –wave interaction

# SAR Imaging of Current Features

- Bragg scattering: Image intensity ∝ Bragg wave intensity
- Wave-current interaction
- Contributions of longer waves
  - Tilt modulation
  - Hydrodynamic modulation
- SAR imaging artifacts
- Further modulation mechanisms

**Courtesy: R. Romeiser Univ. Miami**

# Underwater bottom topography

## San nel

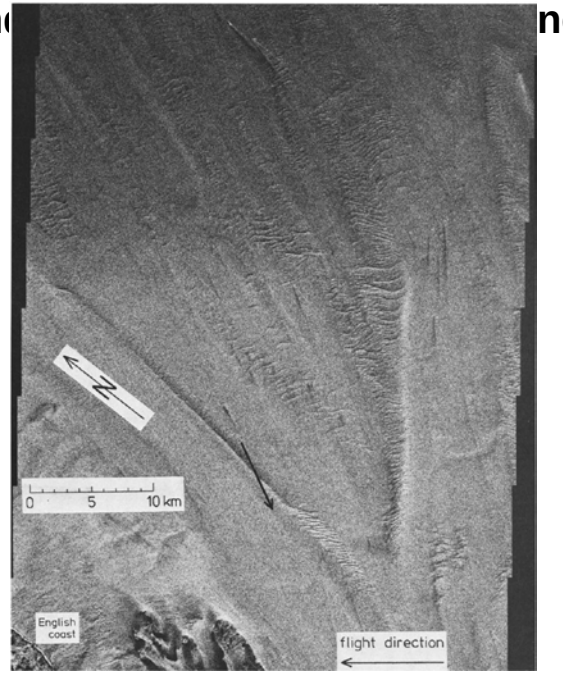


**SEASAT** L-band SAR image of the northeastern approach to the English Channel acquired on 19 Aug 1978 at 0646 UTC. Visible is on the right-hand side the French/Belgian coast. (This image is not corrected for the variation of brightness with incidence angle. This is the reason why the image intensity is high in the lower section of the image corresponding to near range (steep incidence angles). Imaged area:100 km x 100 km.

**Look direction of the antenna**

**Satellite track**

# Other examples of meso-scale oceanic phenomena detectable by SAR:

- Internal waves
- Oceanic fronts
- Upwelling
- Oil pollution
- Oceanic eddies

# Internal waves

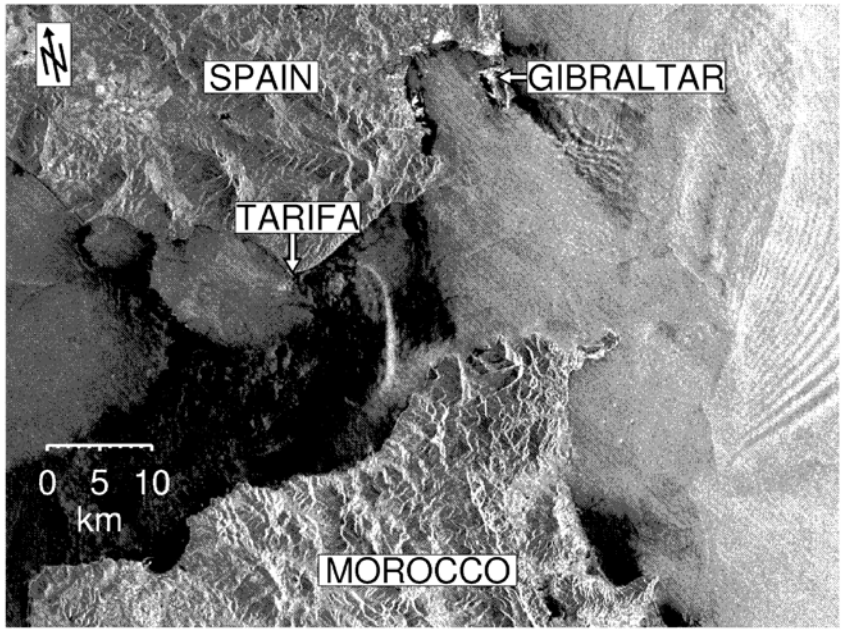


ERS-1 SAR image acquired on 20-01-1994, 11:03 UTC.

Sea surface manifestations of an internal soliton close to its generation area in the center of the strait (bent bright line in the center) and an internal wave packet east of the strait which was generated during the previous tidal cycle. The further away the internal wave packet has propagated from its source, the more solitons are in the packet.

# Bottom topography of the Strait of Gibraltar

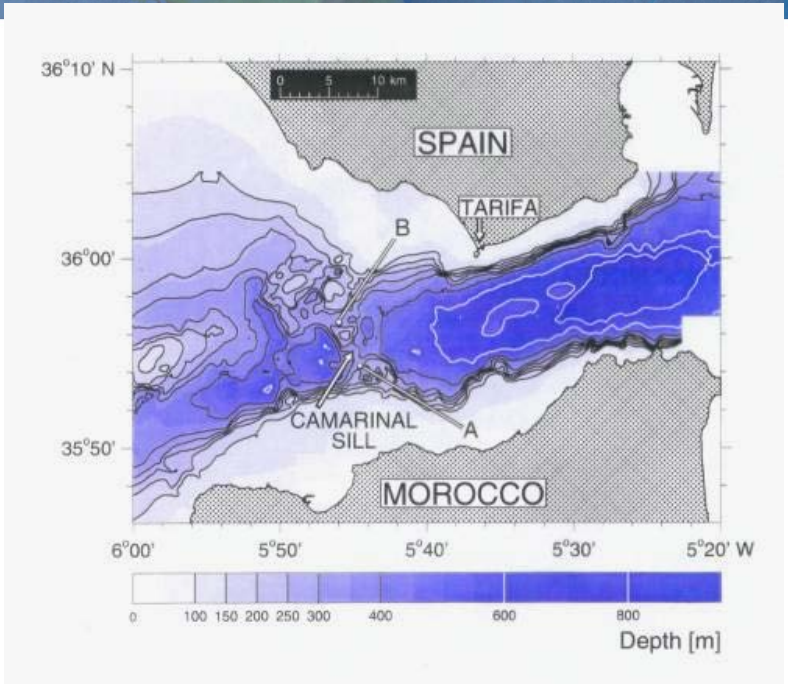


Bottom topography of the Strait of Gibraltar. The shallowest section is at the Camarinal Sill. (Figure reproduced from Brandt, P., Alpers, W. & Backhaus, J. O., Study of the generation and propagation of internal waves in the Strait of Gibraltar using a numerical model and synthetic aperture radar images of the European ERS 1 satellite, *J. Geophys. Res.*, **101**, 14237-14252 (1996)).

# Density distribution of the water column north of the Strait of Messina during the passage of a highly non-linear internal wave packet measured by a thermistor chain towed by the SACLANT research vessel Alliance.

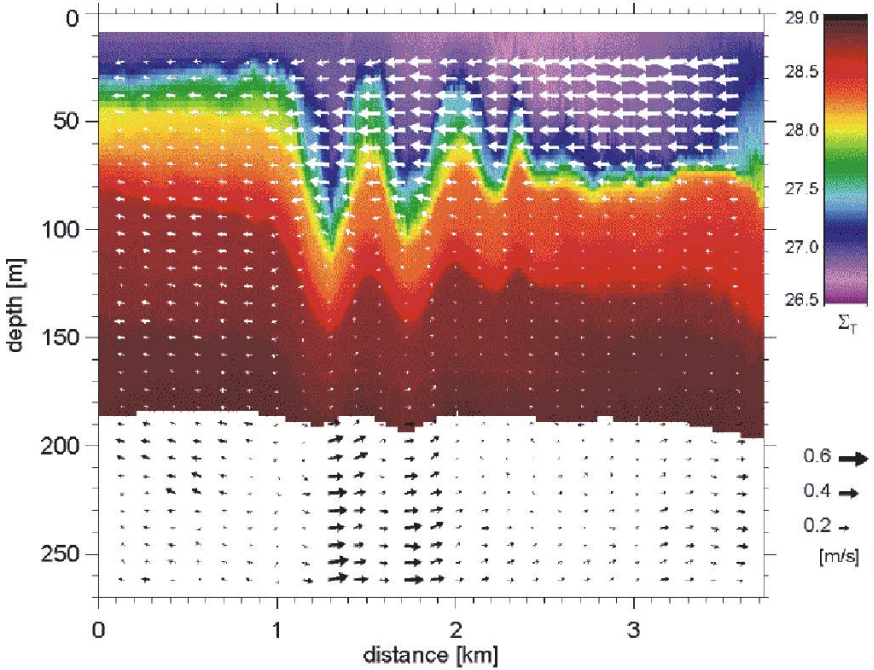

# Why are internal waves visible on the ocean surface?

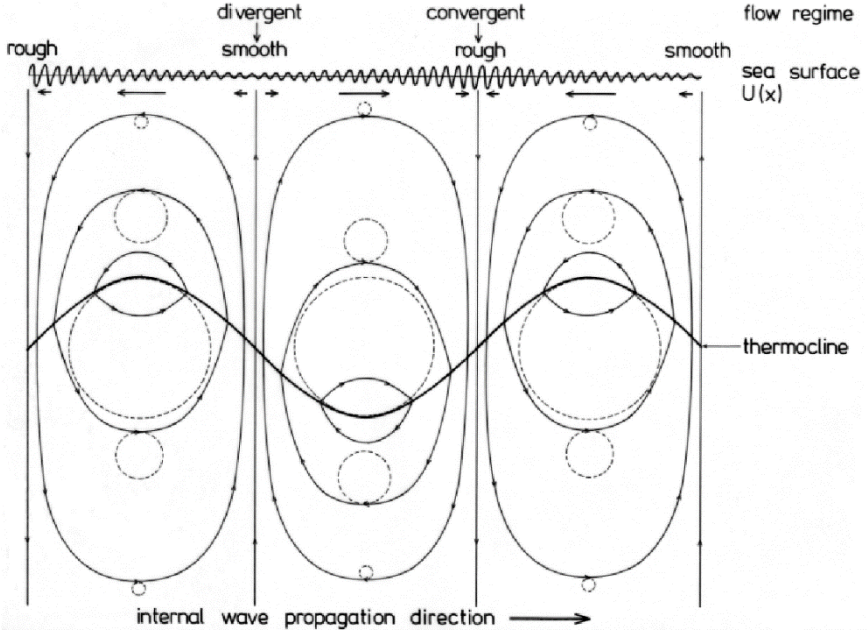


$$\frac{\Delta\sigma}{\sigma_0} = \frac{\sigma - \sigma_0}{\sigma_0} = -A\frac{\partial u_r}{\partial r}$$

**Because internal waves cause small variations of the sea surface velocity, which modulate the short ocean waves ("Bragg waves") responsible for the radar backscattering.**

**$U_r$= horizontal surface velocity in look direction of the SAR antenna (range direction)**

**A = proportionally factor**

Alpers, W.. "Theory of radar imaging of internal waves". *Nature* 314 (1985)

# Sea surface signatures of oceanic internal waves

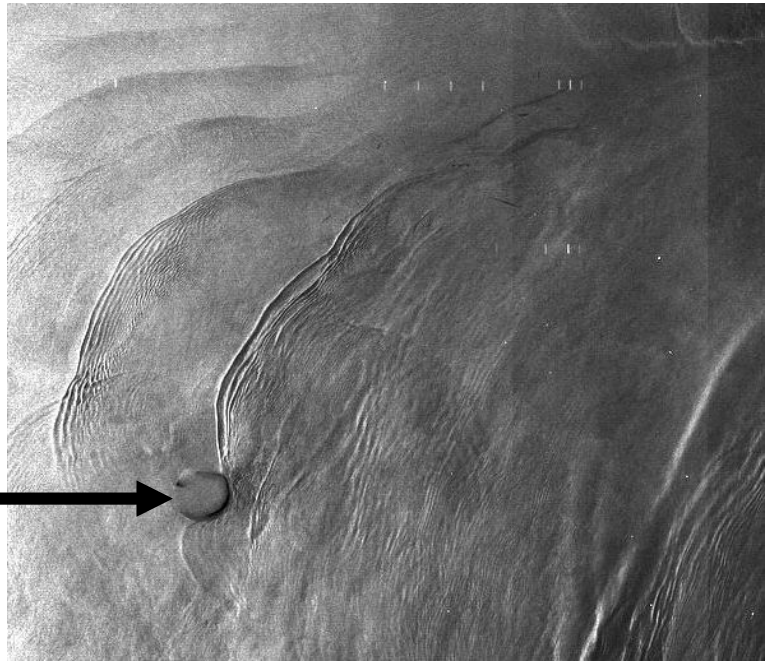


Envisat SAR Wide Swath image acquired over the South China Sea on 18-06-2005, 021:3UTC showing sea surface signatures of oceanic internal waves. Swath widths: 400 km.

# Radar signature of a non-linear internal wave packet consisting of internal solitons of depression

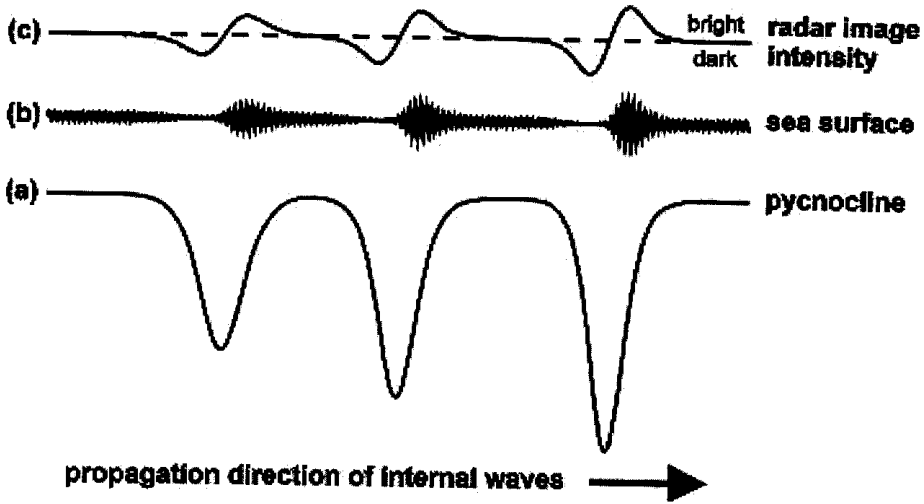

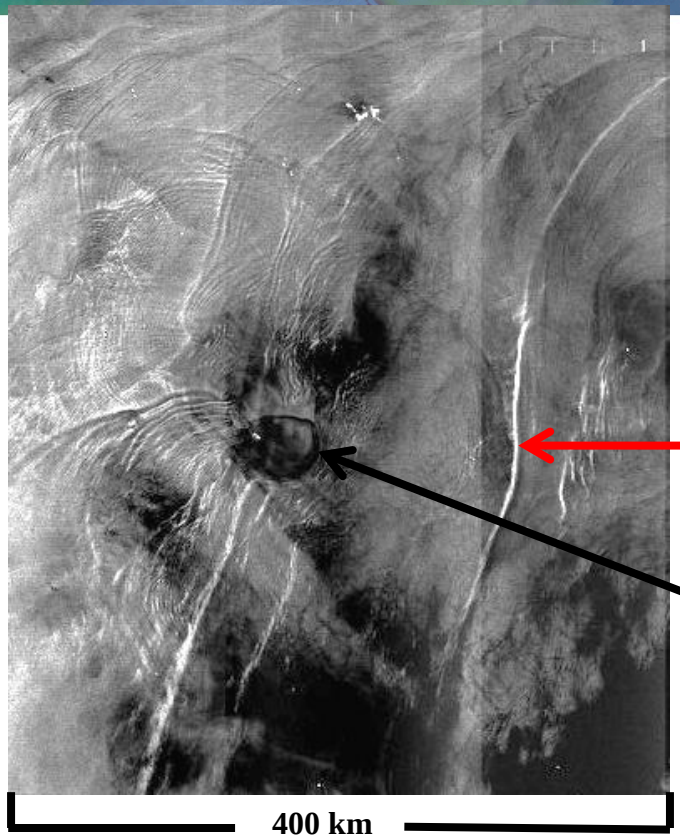


**Envisat SAR WS image of the South China Sea around the Dongsha Atoll showing radar signatures of non-linear internal waves (solitons and wave packets).**

Envisat SAR, 03-11-2005, 14:15 UTC

# Internal waves are also visible on optical images (sunglint images)

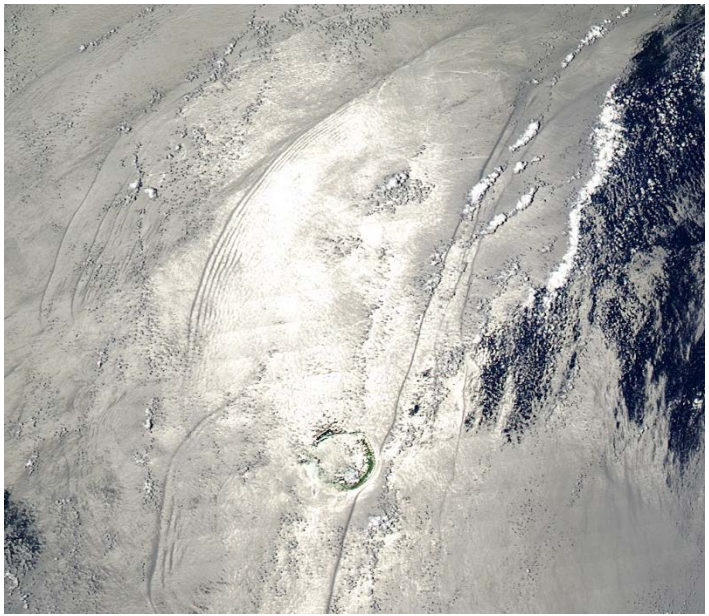

MODIS Aqua image,
03-11-2005,14:15UTC

True-colour image of the northern portion of the South China Sea

# Generation of a secondary internal wave packet

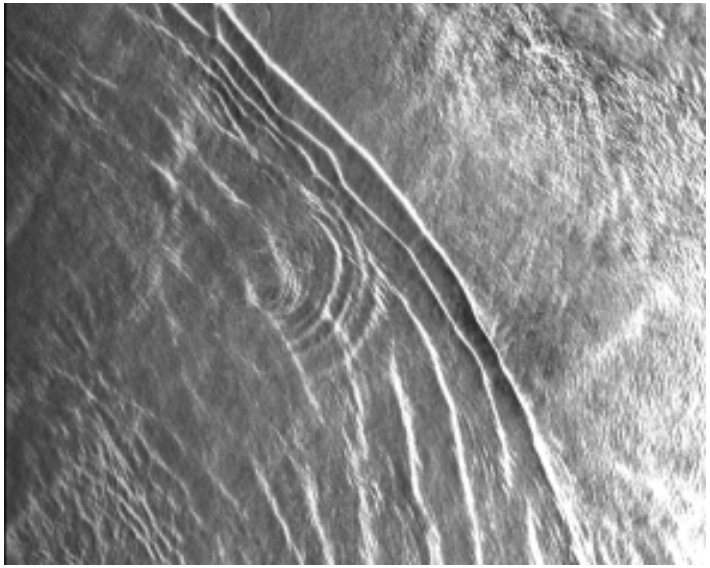

Section of an ERS-2 SAR image acquired over the Andaman Sea showing the generation of secondary internal waves by the interaction of strong internal solitary waves with an underwater sand bank (Dreadnought Bank).in the Andaman Sea The imaged area is 100 km x 80 km.

# Model results

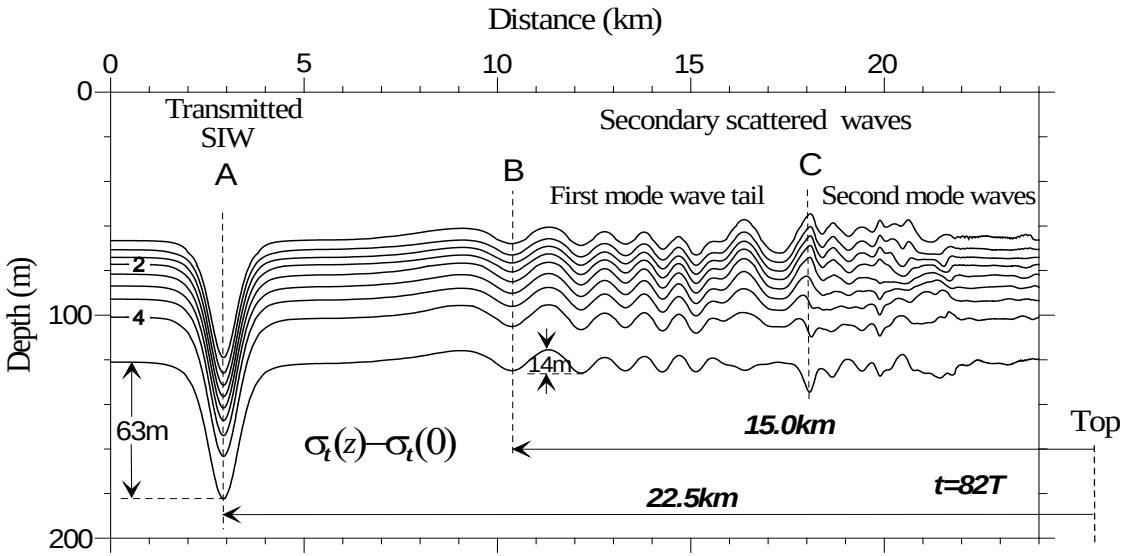


Model result showing the density field anomaly at the time t=82T= 156 s which corresponds to the time at which the ERS SAR image was acquired. The letters A, B and C denote the positions of the transmitted primary ISW, and of the leading solitons in the first and second mode secondary internal wave packets, respectively. The distances, 22.5 km and 15.0 km, refer to the distances from the centre (top) of the Dreadnought Bank (Vlasenko and Alpers, 2005)

# Oceanic fronts

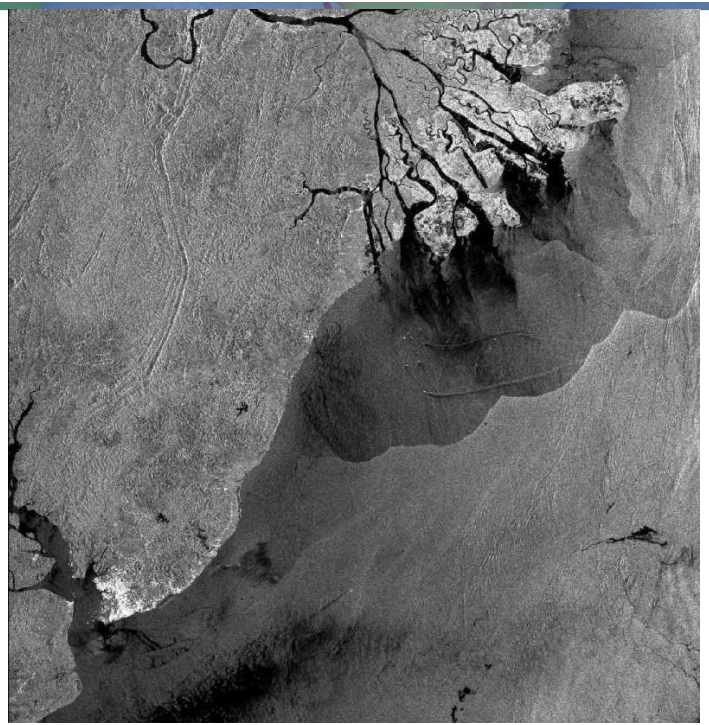

**River outflow**

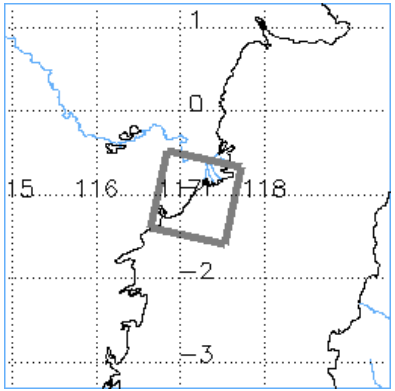


ERS-2 SAR image, 12-12-1999, 02:29 UTC

Frontal boundary between the fresh water outflow from the **river Kutai in Borneo** and the salty water of Macassar Strait. The form of the frontal boundary seems to mirror the water outflow from the various river arms.

# Photo of an oceanic front

# Upwelling

Upwelling areas appear often as dark patches (of reduced NRCS) on SAR images.

The reduction of the NRCS can be caused

- by the change of the stability of the air-sea interface due to upwelled cold water.
  **Typically: $\sigma_0 \leq 3$ dB**

- by biogenic surface films generated by enhanced biota in upwelling regions.
  **Typically: $\sigma_0 = 7 - 12$ dB**

# Upwelling induced by a cyclonic eddy detached from a filament of an upwelling front

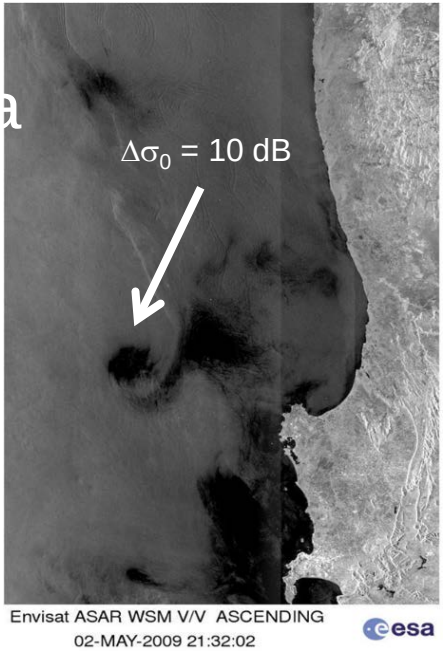


**Black patch is due to biogenic slick**

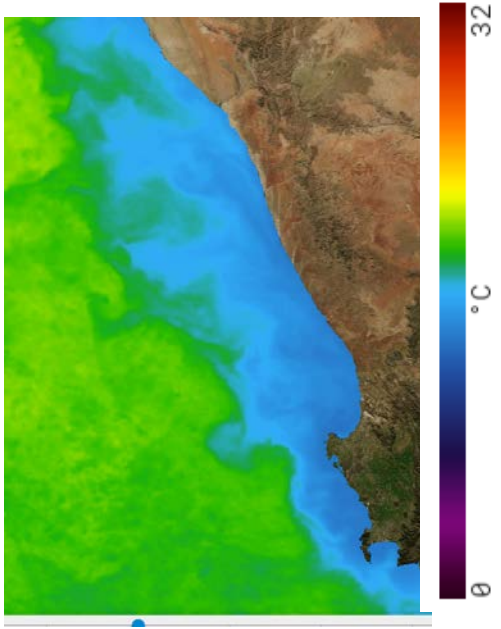


a) Section of an Envisat SAR image acquired **on 2 May 2009** at 21:32 UTC showing part of the west coast of South Africa. B) SST map of 2 May (from MUR) shows west of the diagonal line an area of high SST and east of it an area of high SST caused by cold upwelled water.

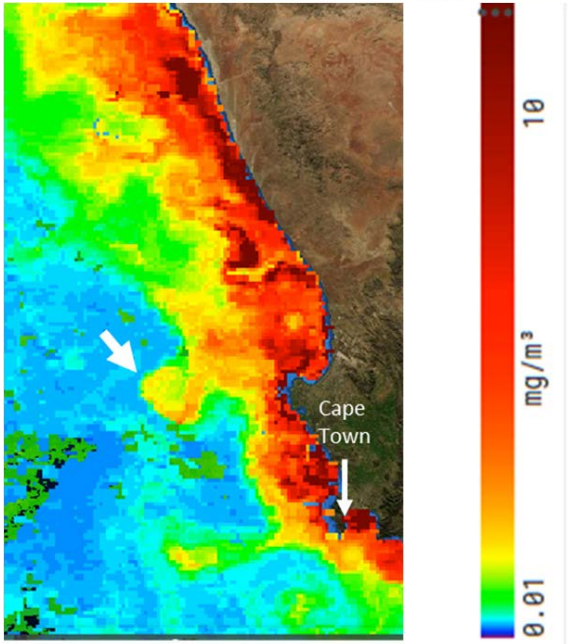





**High Chl-a concentration on the rim of the cyclonic eddy**

**SAR images can be used in synergy with SST and Chl-a images for studying of upwelling**

**Chl-a map derived from the MODIS/Acqua data** (L3 product, 4 km resolution, averaged over 5 days) valid for **5 May 2009** showing a band of enhanced chl-a concentration along the west coast of South Africa and a cyclonic eddy marked by an arrow.

Source: https//podaac-tools.jpl.nasa.gov.

# Oceanic eddies

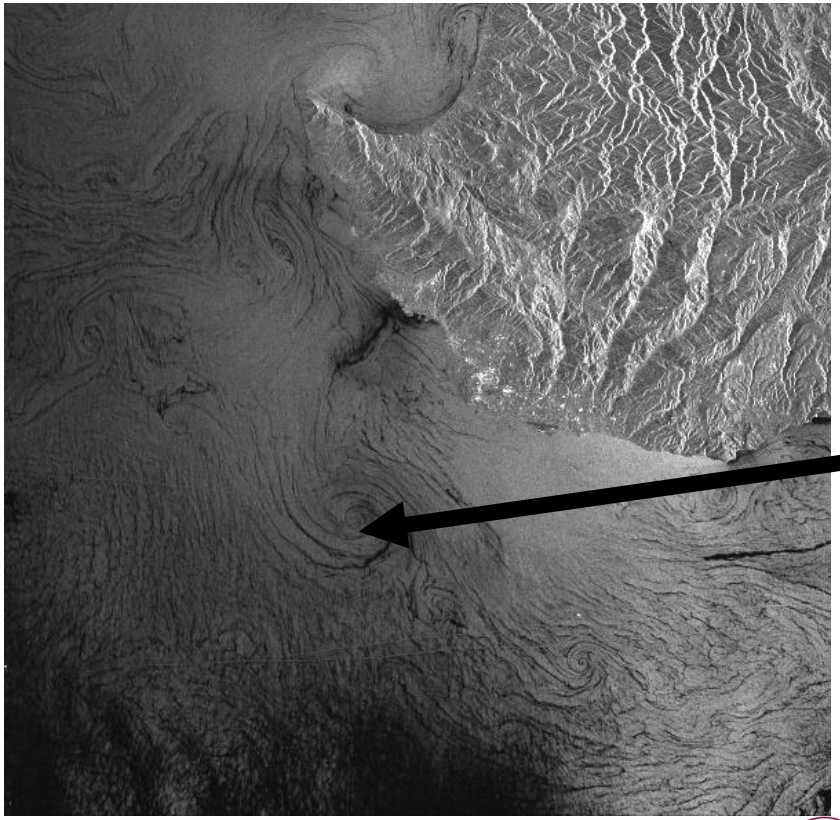


Small-scale oceanic eddies off the **southwestern coast of Cyprus.** The eddies become visible because they entrain surface slicks.

ERS-1 SAR image, 06-10-1994 08:32 UTC, imaged area: 100 km x 100 km.

# Dipole oceanic eddy in the Mediterranean Sea

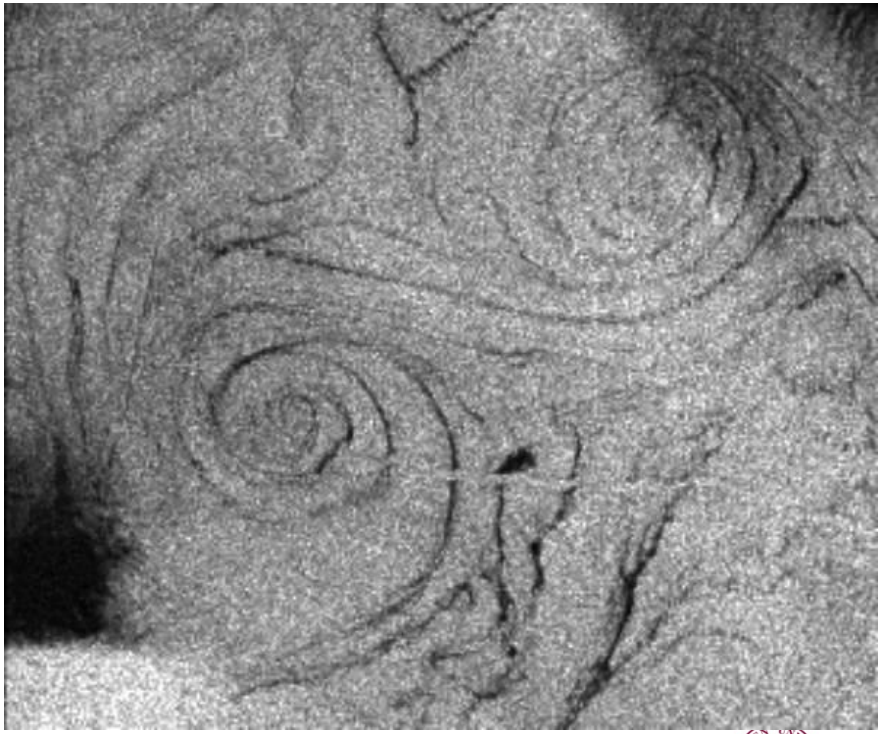

ERS-1 SAR image, 19-09-1993, 9:41 UTC, imaged area: 15 km x 13 km.

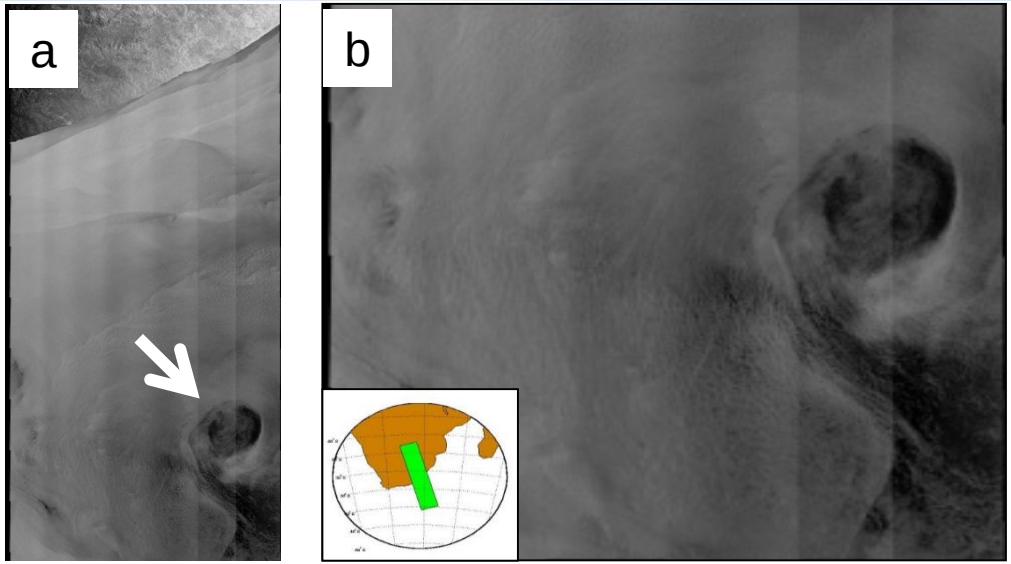


(a) Section of an SAR image acquired by the SAR onboard the Envisat satellite in the Wide Swath Mode (WSM) at 0113 UTC on 06-12-2011 during a ascending satellite pass showing in the lower right-hand section the radar signature of a cyclonic eddy southeast of South Africa. The imaged area is 400 km x 1000 km. (b) Zoom on the eddy whose diameter is approximately 110 km. The inset shows the position of the entire imaged scene.

From Alpers et al., 2004

# Upwelling caused by a meander of the Agulhas Current

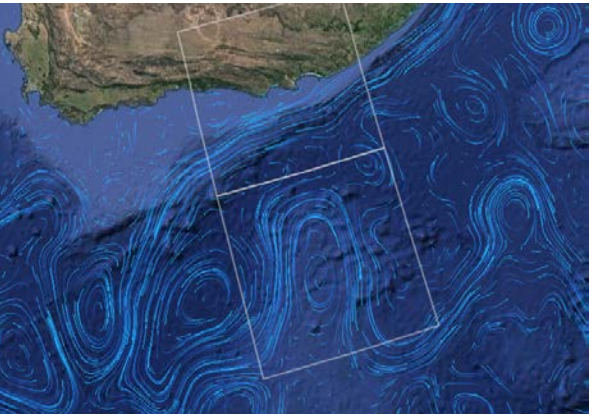

Geostrophic surface current streamlines from Globecurrent

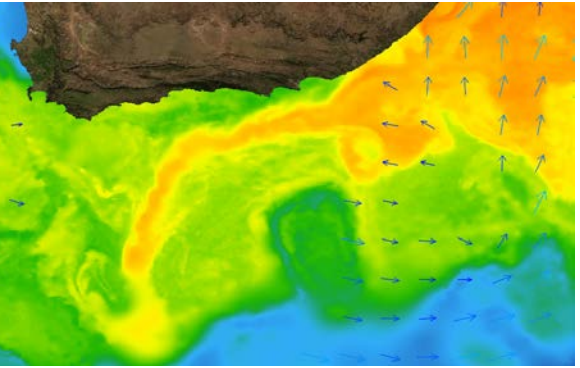

22 Dec 2014

SST from MUR
+ Surface wind from satellite

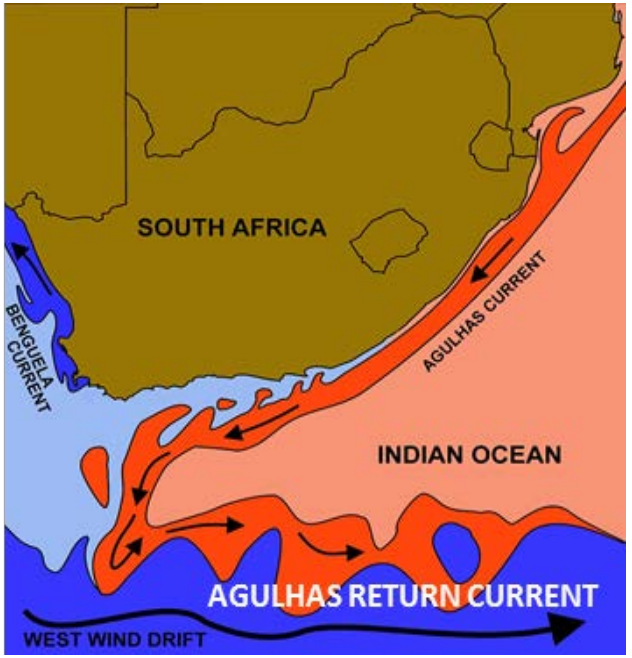


Source: OceanDataLab

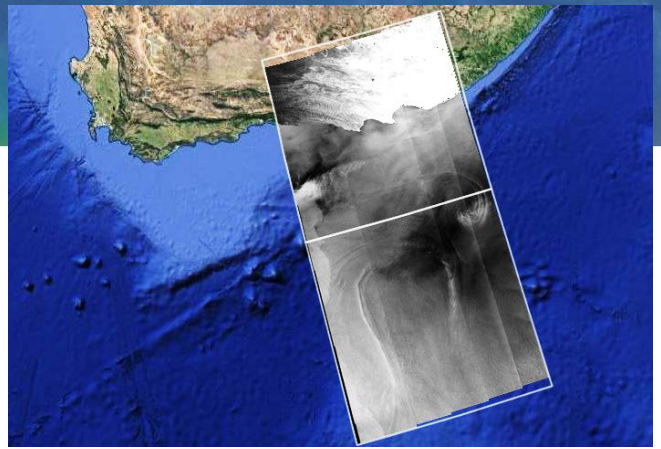

Sentinel-1A image,
22 December 2014

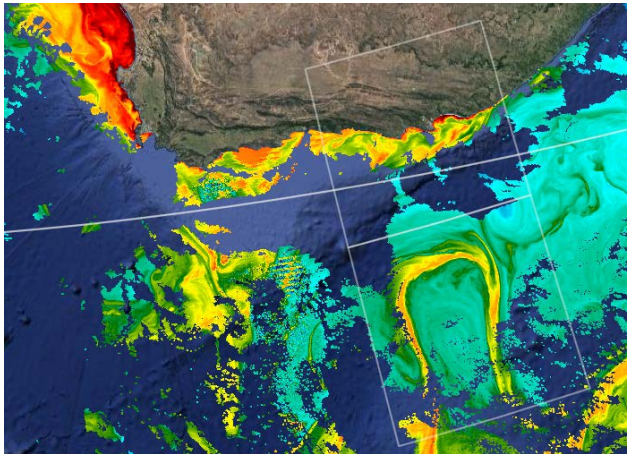

Chl-a concentration,
22 December 2014 from
VIRS (NASA)

Source: OceanDataLab

# Variation of the normalized radar cross section $\sigma_0$ over the meander

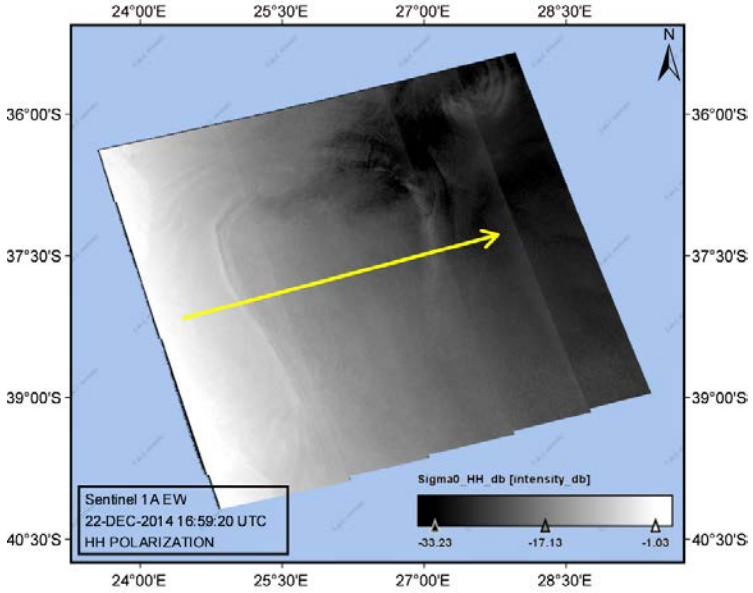


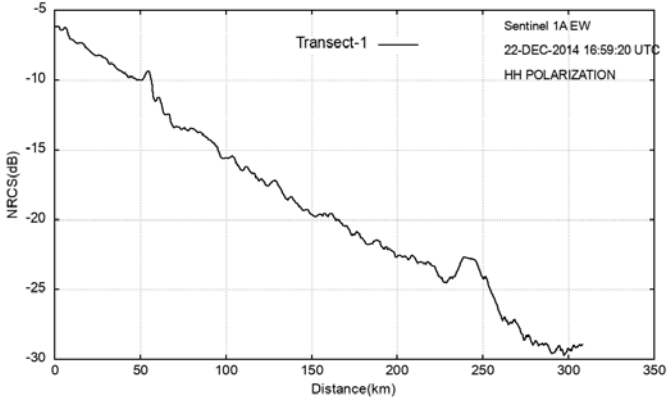


$\Delta\sigma_0 = 0.5$ dB $\Delta\sigma_0 = 2.0$ dB

**SAR images can be used in synergy with SST and Chl-a images for studying of upwelling in meanders.**

# Warm eddy = anti-cyclonic (ac) eddy

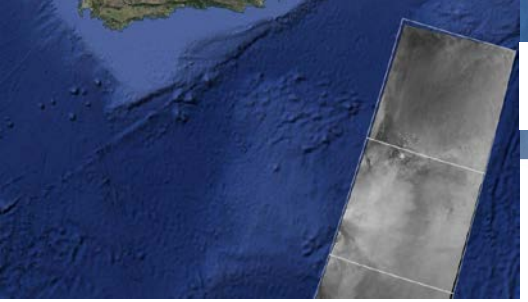

Sentinel-1A,
16 July 2015, 0305 UTC

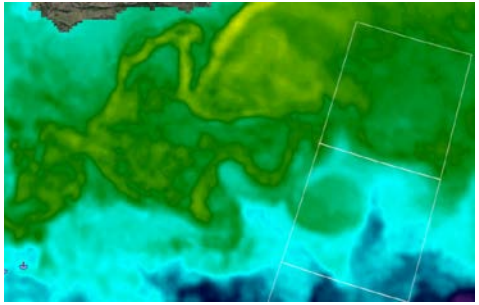

SST from MUR,
16 July 2015

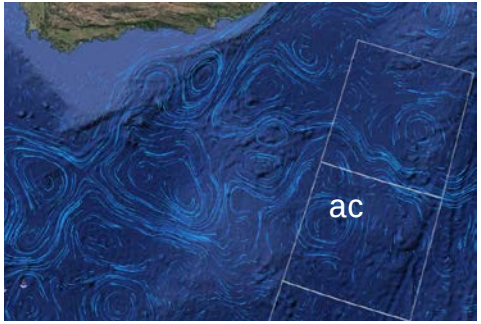


Geostrophic surface current streamlines from Globecurrent

# Oil spill detection

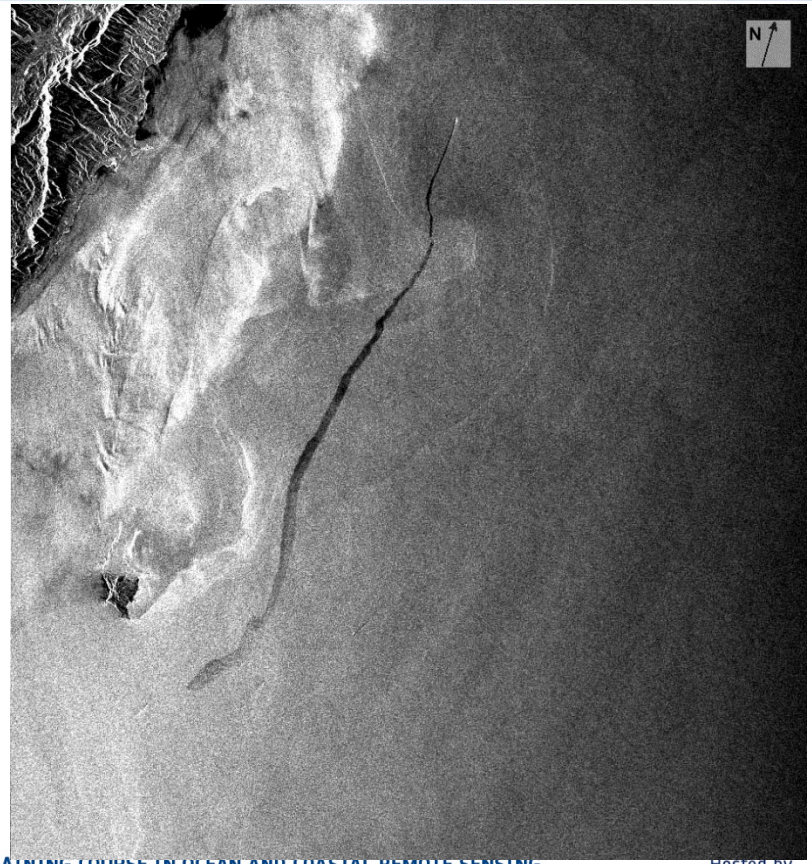


## Ship generated oil spill

ERS-1 SAR image acquired on 20-05-1994,14:20 UTC over the Pacific Ocean east of Taiwan; frame center: 23° 01'N, 121° 41'E, imaged area: 100 km x 100 km.
A ship travelling northward (bright spot at the front of the black line) discharging oil. The oil disperses with time causing the oil trail to widen.

Alpers et al., Remote Sensing of Environment 201 (2017) 133–147

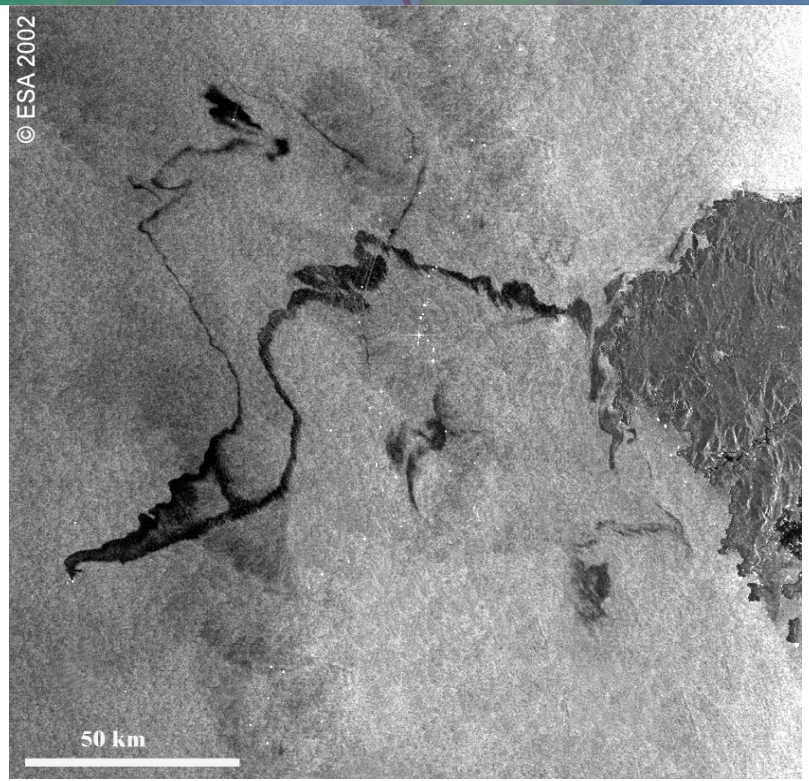


6 – 10 December, 2004

**Oilspill originating from the „Prestige“ tanker accident off the coast of northern Spain**

Envisat ASAR WS image

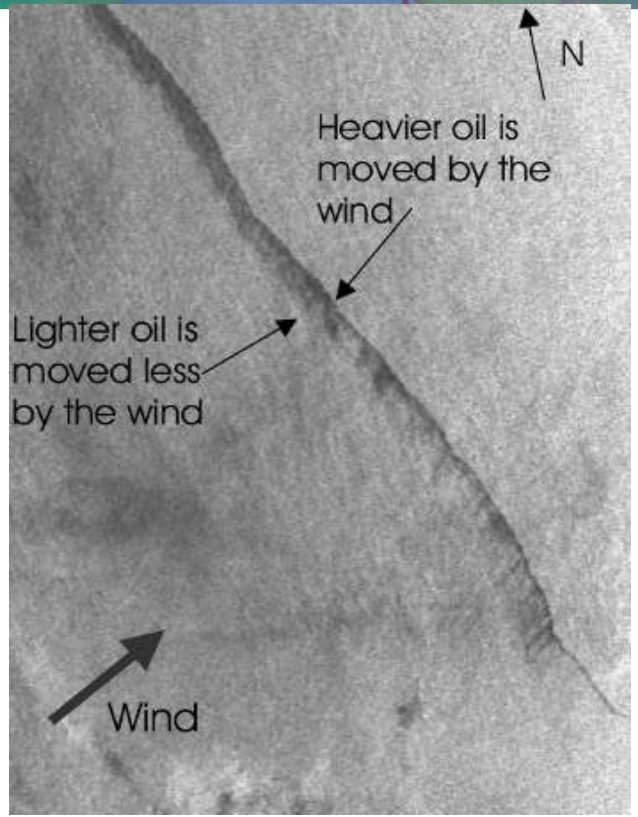


**Section of an ERS-2 SAR image from the Indian Ocean (06-04-1999, 4:58 UTC, 36'N, 81° 49'E) showing a "feathered" structure of an oil trail.**

**By the action of the wind, the heavy components of the mineral oil film accumulate at the downwind side (dark line in the image). The "feathered" side is always located upwind.**

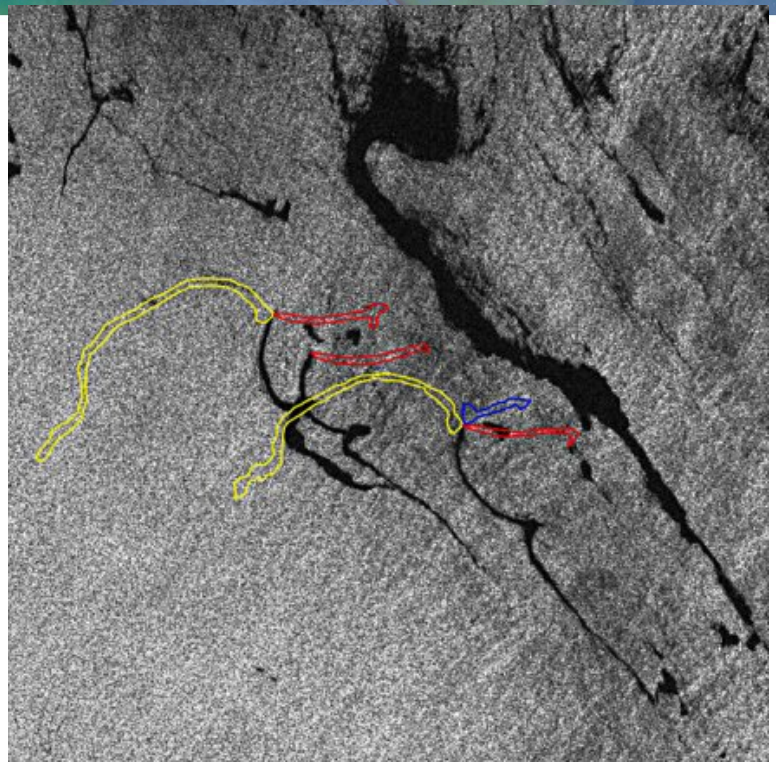

Source: http://www.infoterra-global.com/explore/natseep.htm

## Locating oil seeps on sequences of SAR images

The image shows multiple streaming oil slicks in the South Caspian Sea. The colour vector overlays show the position of the slicks from previous data acquistions over a ten year period. The presence of repeating slicks with the same point source increases the confidence that there is a natural oil seep source for these slicks. The only alternative would be a sunken ship leaking oil. Ground truthing can confirm the source of the seepage

# Dark patches on SAR images of the ocean surface do not always originate from mineral oil films.

**They can also originate from:**

- natural surface films which are produced by plankton or fish
- low winds which are often encountered in the lee of islands or coastal mountains
- cold upwelling water which changes the stability of the air-sea interface
- divergent flow regimes associated, e.g., with internal waves or tidal flow over sand banks
- dry fallen sand banks
- turbulent water as encountered in ship wakes
- grease ice

**“Oil spill Look-alikes”**

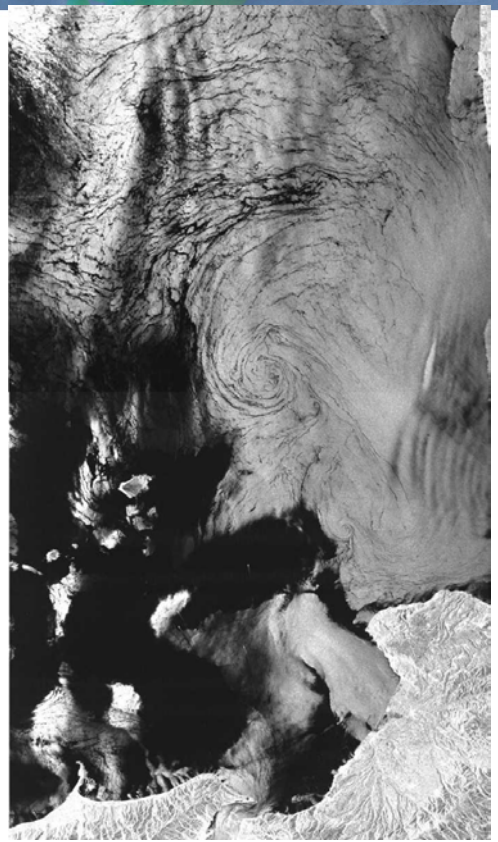

## Natural surface films (biogenic slicks)

ERS-SAR image,
03-06-1994, 21:13 UTC,
Mediterranean Sea, north of Sicily

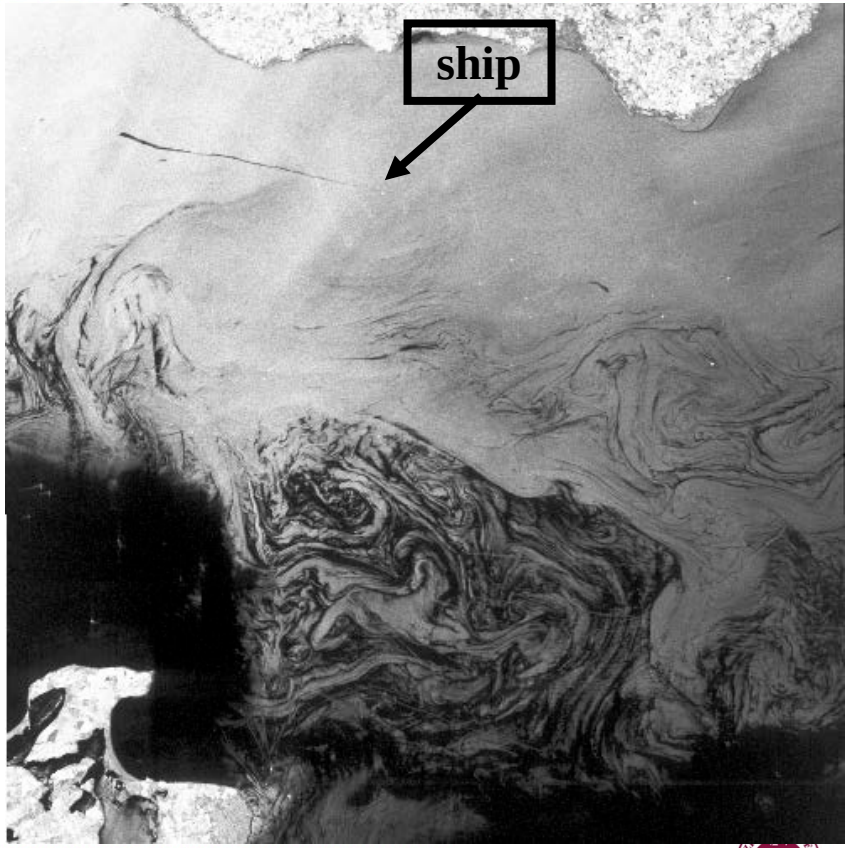


## Natural surface films (biogenic slicks)

ERS-1 SAR image acquired over the Baltic Sea (Pommerian Bight) on 16-04-1994, 21:04 UTC


ERS-2 image acquired on 12-10- 1993, 18:54 UTC;
imaged area: 100 km x 100 km .

## Natural surface films (biogenic slicks)

**Eddies in the Caspian Sea south of the Volga estuary.**

The oceanic eddies, which become visible on the radar image because the surface slicks (biogenic slicks) follow the surface currents, are very likely wind-induced.

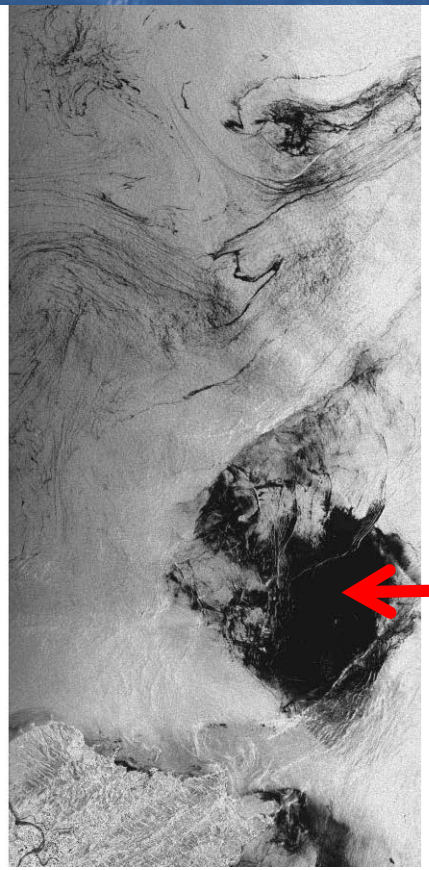

**ERS-1 SAR**
**23 July, 1994**

**Upwelling**
**Area North of**
**Taiwan**

Dark area associated with upwelling

# Chlorophyll-a concentration, East China Sea

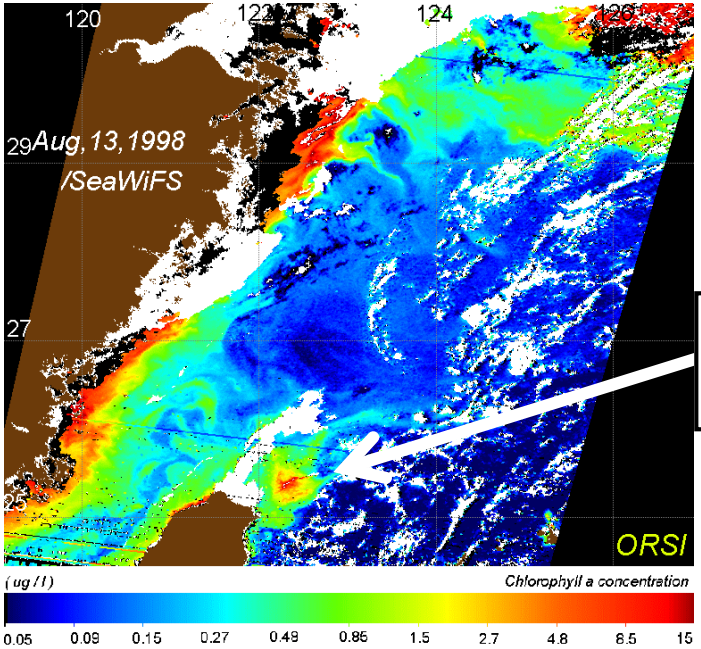


**Upwelling area north of Taiwan**

# Conclusion

- Microwaves do not penetrate into the water body.
- SAR can detect oceanic phenomena only indirectly via variations of the sea surface roughness.
- Only when the oceanic phenomena below the sea surface are associated with variable surface currents, which modulate the short-scale sea surface roughness, they become detectable by SAR.
- When combined with data from other sensors and with model outputs, SAR images of the sea surface can contribute significantly to understand better the dynamics of meso-scale oceanic phenomena, like internal waves.

More examples can be found at

https://earth.esa.int/web/guest/-/ers-sar-tropical-5883:

“The tropical and subtropical ocean viewed by ERS SAR”

by

Werner Alpers, Hamburg
Leonid Mitnik, Vladivostok
Lim Hock, Singapore
Kun Kan Chen, Chungli, Taiwan

Thank you for your attention

谢谢！